

# Production of CO<sub>2</sub> in Soil Profiles of a California Annual Grassland

Noah Fierer,<sup>1\*</sup> Oliver A. Chadwick,<sup>2</sup> and Susan E. Trumbore<sup>3</sup>

<sup>1</sup>Department of Biology, Duke University, Durham, North Carolina 27708, USA; <sup>2</sup>Department of Geography, University of California, Santa Barbara, California 93106, USA; <sup>3</sup>Department of Earth System Science, University of California, Irvine, California 92697, USA

## ABSTRACT

Soils play a key role in the global cycling of carbon (C), storing organic C, and releasing CO<sub>2</sub> to the atmosphere. Although a large number of studies have focused on the CO<sub>2</sub> flux at the soil–air interface, relatively few studies have examined the rates of CO<sub>2</sub> production in individual layers of a soil profile. Deeper soil horizons often have high concentrations of CO<sub>2</sub> in the soil air, but the sources of this CO<sub>2</sub> and the spatiotemporal dynamics of CO<sub>2</sub> production throughout the soil profile are poorly understood. We studied CO<sub>2</sub> dynamics in six soil profiles arrayed across a grassland hillslope in coastal southern California. Gas probes were installed in each profile and gas samples were collected weekly or biweekly over a three-year period. Using soil air CO<sub>2</sub> concentration data and a model based on Fick's law of diffusion, we modeled the rates of CO<sub>2</sub> production with soil profile depth. The CO<sub>2</sub> diffusion constants were checked for accuracy using measured soil air <sup>222</sup>Rn activities. The modeled net CO<sub>2</sub> production rates were compared with CO<sub>2</sub> fluxes measured at the soil surface. In general, the modeled and measured net CO<sub>2</sub> fluxes were very similar although the model consistently underestimated CO<sub>2</sub> production rates in the surficial soil horizons when the soils were moist. Profile

CO<sub>2</sub> production rates were strongly affected by the inter- and intra-annual variability in rainfall; rates were generally 2–10 times higher in the wet season (December to May) than in the dry season (June to November). The El Niño event of 1997–1998, which brought above-average levels of rainfall to the study site, significantly increased CO<sub>2</sub> production in both the surface and subsurface soil horizons. Whole profile CO<sub>2</sub> production rates were approximately three times higher during the El Niño year than in the following years of near-average rainfall. During the dry season, when the net rates of CO<sub>2</sub> flux from the soil profiles are relatively low (4–11 mg C–CO<sub>2</sub> m<sup>-2</sup> h<sup>-1</sup>), 20%–50% of the CO<sub>2</sub> diffusing out of the profiles appears to originate in the relatively moist soil subsurface (defined here as those horizons below 40 cm in depth). The natural abundance <sup>14</sup>C signatures of the CO<sub>2</sub> and soil organic C suggest that the subsurface CO<sub>2</sub> is derived from the microbial mineralization of recent organic C, possibly dissolved organic C transported to the subsurface horizons during the wet season.

**Key words:** soil carbon; soil respiration; CO<sub>2</sub> flux; <sup>14</sup>C; belowground processes; vadose zone processes.

## INTRODUCTION

Worldwide, soils store approximately 1600 Pg of organic carbon (C) (Eswaran and others 1993), an amount of C more than two times greater than that stored in the atmosphere. Soils are also a major

source of atmospheric CO<sub>2</sub>, contributing 60–70 Pg CO<sub>2</sub>–C per year (Schimel 1995). The balance between soil organic C storage and soil CO<sub>2</sub> production has a major influence on atmospheric CO<sub>2</sub> concentrations (Schlesinger 1991).

Although a majority of soil CO<sub>2</sub> production occurs in the organic-rich surface horizons (deJong and Schappert 1972; Davidson and Trumbore 1995; Gaudinski and others 2000; Elberling 2003), the

Received 13 October 2003; accepted 6 February 2004; published online 28 June 2005.

\*Corresponding author; e-mail: fierer@lifesci.ucsb.edu

rates of CO<sub>2</sub> production in subsurface, mineral horizons can be significant (Wood and Petraitis 1984; Ajwa and others 1998; Keller and Bacon 1998; Hendry and others 1999; Pumpanen and others 2003). Relatively few studies have examined the environmental controls on the production and transport of CO<sub>2</sub> in the deeper soil horizons. Because a large portion of the organic C stored in soil resides in deeper soil horizons (Batjes 1996), even small changes in the rate of organic C mineralization within subsurface horizons could have significant effects on atmospheric CO<sub>2</sub> concentrations and global C dynamics.

Few studies have examined the production and transport of CO<sub>2</sub> within and between individual soil horizons. The majority of studies on soil CO<sub>2</sub> production focus on the net flux of CO<sub>2</sub> across the soil/atmosphere interface, integrating CO<sub>2</sub> fluxes from all the layers of a given soil profile, but providing little information on the distribution of CO<sub>2</sub> production within soil profiles. We know that the concentrations of CO<sub>2</sub> in deeper soil horizons are often very high (Amundson and Davidson 1990; Burton and Beauchamp 1994; Hendry and others 1999), which could result from high CO<sub>2</sub> production rates, low rates of CO<sub>2</sub> diffusion out of the subsurface horizons, or some combination of the two. The dynamics of CO<sub>2</sub> production and its diffusion through soil profiles represent large sources of uncertainty in studies of terrestrial ecosystem carbon cycling (Schimel and others 1994; Billings 1995) and pedogenesis (Solomon and Cerling 1987; Richter and Markewitz 1995; Andrews and Schlesinger 2001).

In any given soil horizon, the rate of biotic CO<sub>2</sub> production will largely be a function of four factors: plant root activity and abundances, water availability to microorganisms, soil temperature, and resource (primarily C) supply to microorganisms (Schimel and others 1994; Rustad and others 2000; Chapin and others 2002). The rate of CO<sub>2</sub> movement within a soil profile, or to the soil–air interface, is determined by the physical properties of the profile, including (but not limited to) air-filled porosity, the connectivity of the air-filled pore spaces, and the CO<sub>2</sub> concentration gradient (Thorstenson and Pollock 1989; Hillel 1998). These biotic and abiotic controls on soil profile CO<sub>2</sub> production and transport can change significantly over time (Solomon and Cerling 1987; Amundson and Davidson 1990; Elberling 2003), particularly in semiarid ecosystems where the inter- and intra-annual variability in precipitation is often very high (Rambal and Debussche 1995; Chamran and others 2002). For this reason, any study of soil C dynamics in semiarid

ecosystems must explicitly consider the effects of precipitation patterns on soil CO<sub>2</sub> dynamics.

Between 1997 and 2001, we measured soil air CO<sub>2</sub> concentrations in a series of profiles arrayed across a grassland hillslope in coastal southern California. A high level of interannual variability in rainfall patterns was observed over the three-year study, the El Niño event of 1997–1998 resulted in significantly above-average amounts of rainfall. We used the soil air CO<sub>2</sub> concentration data and estimates of soil gas diffusion rates to estimate CO<sub>2</sub> production rates in each of the six studied soil profiles. Our estimates of gaseous diffusion rates through the profiles were constrained by soil air <sup>222</sup>Rn concentrations. The model estimates of net CO<sub>2</sub> flux to the atmosphere from each profile were compared with CO<sub>2</sub> fluxes measured at the soil surface. We used <sup>14</sup>C analyses of soil organic carbon and soil CO<sub>2</sub> to identify the potential sources of CO<sub>2</sub> within the studied profiles.

## METHODS

### Study Area

The study was conducted at the University of California Sedgwick Reserve (34°42'N, 120°03'W) located 50 km north of Santa Barbara, California, USA, in the Santa Ynez Valley. The study site was a 2-ha hillslope catena extending 30 m in elevation from valley-bottom to ridge-top. The hillslope is on a southwest-facing slope of a planar fluvial terrace underlain by the Paso Robles formation, a weakly consolidated early Pleistocene alluvium composed largely of Monterey shale (Dibblee 1966). There is no incised drainage and no indication of overland fluvial transport at the site, even on the steepest portions of the catena. The hydrology and pedology of the hillslope have been described in previous studies (Gessler and others 2000; Chamran and others 2002). The vegetation at the site is dominated by annual Mediterranean grasses (*Bromus* spp., *Avena* spp., and *Vulpia myuros*) with several perennial blue oaks (*Quercus douglasii*) and coast live oaks (*Quercus agrifolia*) sparsely distributed across the hillslope. On average, the annual grasses germinate in November and senesce in May.

Six sampling locations were chosen across the hillslope for soil profile characterization and instrumentation (Figure 1). The studied profiles are located in shoulder, concave, or toe slope positions. Soils in the concave and toe slope positions (Profiles 10, 14, 18, and 19) accumulate water and sediment at higher rates than soils in the relatively stable shoulder positions (Profiles 2 and 4), where soil formation is largely in situ. The profiles are not

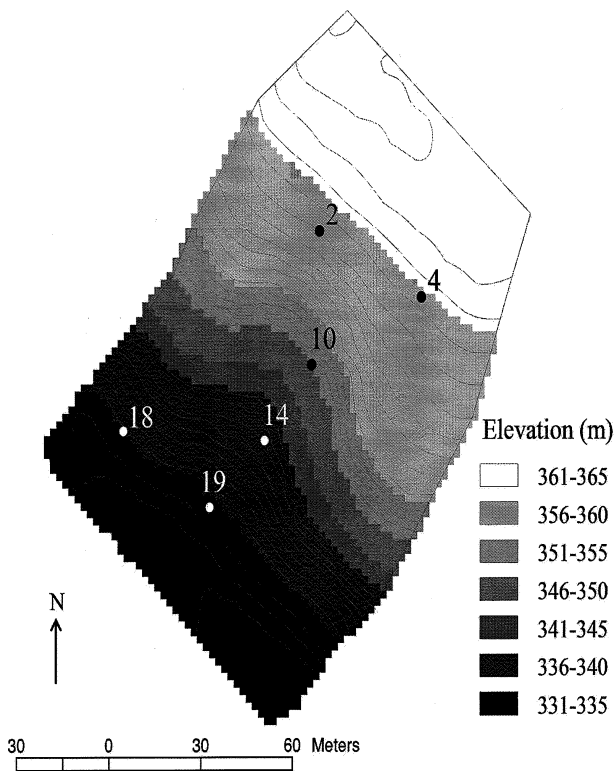


Figure 1. Digital elevation model of the hill-slope with locations of the instrumented profiles indicated.

numbered consecutively because we did not include any sampling locations on convex slopes where soil depths were too shallow to permit adequate calculation of  $\text{CO}_2$  fluxes from the profile  $\text{CO}_2$  concentration data. The selected profiles vary significantly in terms of soil type, A horizon depth, and total soil depth (Table 1). Additional information on the study site and the specific sampling locations can be found in Gessler and others (2000).

The site is characterized by a Mediterranean-type climate with hot, dry summers and cool, moist winters. Annual precipitation is highly variable; the average annual rainfall between 1990 and 2000 was  $50 \text{ cm y}^{-1}$ . Precipitation data for the field site was obtained from the records of the Cachuma Lake NOAA weather station, located approximately 15 km from the field site. The average monthly precipitation data for the study period is given in Figure 2. Over the three-year study period, air temperatures ranged from  $6^\circ\text{C}$  to  $40^\circ\text{C}$  (annual average =  $22^\circ\text{C}$ ).

### Profile Characterization

In April 1997 the six soil profiles were excavated down to 3–4 m (or to the C horizon, depending on the soil depth) and described using standard procedures (Soil Survey Staff 1996a). Soil samples were

collected from each major horizon and transported to the University of California at Santa Barbara for chemical and particle-size analyses. Samples were oven-dried, crushed, and sieved to 2 mm; all particle-size and chemical analyses were conducted on the less than 2 mm fraction. Total carbon and nitrogen content was measured with a Fisons NA1500 C/N analyzer. Particle size and soil pH analyses were completed by the University of Missouri Soil Analysis Lab using standard methods. Bulk density was measured on several intact clods per horizon, using the saran-coated clod method (Soil Survey Staff 1996b). The total mass of C in each profile was calculated by multiplying the measured C contents for each horizon by the bulk density of the horizon, correcting for gravel content, and multiplying the mass of C in each soil horizon by horizon thickness. Inorganic C contents in these soils are very low ( $< 0.01\%$  inorganic C by weight; Fierer unpublished data) so we assume that total C concentrations are equivalent to organic C concentrations. The aboveground net primary productivity of grasses at each profile location was determined in April 1997, at the height of the annual growing season, by clipping plots ( $0.1 \text{ m}^2$  in size) to bare ground and weighing the mass of oven-dried plant biomass. Tree biomass was not included in the estimates of net primary productivity because of the limited areal coverage of trees on the hillslope.

### Profile Instrumentation and Monitoring

In April 1997 the excavated soil profiles were instrumented with probes to monitor in situ soil  $\text{CO}_2$  concentrations, soil water contents, and soil temperatures in each of the major soil horizons. Probes were installed through small holes drilled 50 cm into the pit face, parallel to the soil surface and upslope of the excavated profile. In each identifiable soil horizon (Table 1), we placed a complete set of probes: thermocouples to measure soil temperature, buriable three-prong Time Domain Reflectometer (TDR) probes (Soilmoisture Equipment, Santa Barbara, CA) for the measurement of volumetric soil moisture contents, and stainless-steel gas tubes (5 mm o.d., perforated at the end, and inserted approximately 30 cm into the soil pit face) for the collection of soil air samples. The soil pits were carefully back-filled, with the tubes and wires of the instrumentation protected by a vertical PVC conduit leading to the surface.

Data collection started in November 1997 and continued until June 2001. Soil moisture data, temperature data, and soil gas samples were collected weekly during the wet season (December to

**Table 1.** Selected Physical and Chemical Properties of the Studied Soil Profiles, Landscape Position, and other General Characteristics

Profile No.	<2-mm size fraction										Profile and Site Characterization			
	Horizon	Lower horizon depth (cm)	Clay (%)	Silt (%)	Sand (%)	Organic C (%)	pH (H <sub>2</sub> O)	Gravel (%)	Bulk density ( $\rho_b$ ) (g cm <sup>-3</sup> )	A horizon depth (cm)	Depth to C horizon (cm)	Profile C mass (kg m <sup>-2</sup> )	Site NPP (g cm <sup>-2</sup> )	
2	A	3	28.4	33	38.7	1.61	6.5	35.3	0.90	28	85	6	200	
2	ABt1	14	23.9	37.1	38.9	1.88	6.3	33.8	1.87	Typic Argixeroll				
2	ABt2	28	27.2	35.7	37.2	1.12	6.4	50.8	1.65	slope position: shoulder				
2	Bt1	45	42.2	13.2	44.6	0.64	6.3	34.4	1.65					
2	Bt2	85	37.7	13.9	48.4	0.42	6.3	60.1	1.65					
4	A1	6	25.2	41.3	33.5	2.12	6.3	19.6	0.72	31	120	12	548	
4	A2	17	26.4	40.2	33.4	1.14	6.4	28.6	1.95	Typic Argixeroll				
4	AB	31	26.9	38.9	34.1	2.15	6.4	26	2.01	slope position: shoulder				
4	Bt1	52	47.4	32.3	20.3	0.57	6.3	24.3	1.65					
4	Bt2	80	39	36.1	25	0.36	6.6	22.2	1.63					
4	Bt3	120	36	45.4	18.5	0.24	6.9	23.5	1.63					
10	A1	5	25.2	38.9	36	4.14	6.9	59.5	1.05	78	300	20	826	
10	A2	30	28.8	38.5	32.7	1.78	6.7	35.6	1.59	Paehic Haploxeroll				
10	AB1	53	34.1	34.8	31.1	0.87	6.8	37.2	1.41	slope position: colluvial hollow				
10	AB2	78	35.3	34.7	30	0.67	6.9	30.6	1.69					
10	BA	113	36.4	33.7	29.9	0.58	6.9	31.4	1.54					
10	B1	162	35.6	35	29.3	0.42	7.1	37.5	1.52					
10	B2	205	34.9	34.4	30.7	0.35	7.2	37	1.55					
10	BC	300	33.3	35.8	30.9	0.23	7.3	32.5	1.59					
14	A1	5	29.6	40.5	29.9	2.61	6.8	45.3	1.20	63	365	19	337	
14	A2	16	29.6	42.9	27.4	1.63	6.6	38.5	1.40	Paehic Haploxeroll				
14	A3	32	32.7	41.6	25.6	1.24	6.6	27.6	1.63	slope position: colluvial hollow				
14	AB	63	38.8	36.2	24.9	0.91	6.7	39.7	1.69					
14	BA1	92	44.2	31.6	24.2	0.64	6.7	29.8	1.73					
14	BA2	130	39.7	34	26.3	0.46	6.9	32.5	1.78					
14	B1	176	38.4	34.2	27.4	0.32	7.1	36	1.68					
14	B2	365	37.5	35.1	27.4	0.23	7.3	33.5	1.64					
18	A1	3	30.3	42.4	27.3	1.16	7.3	27.8	1.64	80	160	12	309	
18	A2	7	30.2	42.5	27.2	1.34	6.9	22.6	1.57	Paehic Haploxeroll				
18	A3	42	32.8	39.2	28	1.16	6.9	30.1	1.62	slope position: toe slope				
18	AB	66	35.5	39.1	25.4	0.74	7.2	22.6	1.63					
18	BA	90	35.6	39.6	24.8	0.61	7.3	34.2	1.63					
18	B1	126	35.2	39.7	25.1	0.48	7.5	27.6	1.63					
19	A1	5	26.8	42.5	30.7	3.87	6.5	46.3	1.20	45	457	20	636	
19	A2	24	28.4	43	28.6	1.67	6.7	40.1	1.45	Paehic Haploxeroll				

Table 1. Continued

Profile No.	Lower horizon depth (cm)	<2-mm size fraction							Profile and Site Characterization			
		Horizon	Clay (%)	Silt (%)	Sand (%)	Organic C (%)	pH (H <sub>2</sub> O)	Gravel (%)	Bulk density (ρ <sub>b</sub> ) (g cm <sup>-3</sup> )	A horizon depth (cm)	Depth to C horizon (cm)	Profile C mass (kg m <sup>-2</sup> )
19	40	A3	31.2	40.3	28.5	1.31	6.7	29.3	1.62	slope position: bottom of colluvial hollow		
19	80	AB1	39.2	35.8	25	0.94	6.8	34.1	1.83			
19	122	BA/B1	39.7	32.7	27.6	0.58	7.1	58.7	1.87			
19	158	B2	35.8	34.1	30.2	0.42	7.2	43.6	2.06			
19	300	B	31	32.1	36.9	0.21	7.3	46.5	1.71			

NPP is net annual primary productivity of aboveground vegetation.

May) and twice a month during the dry season (June to November). Soil gas samples (10 mL in volume) were collected after removing and discarding 20 mL of air from the gas probes. Gas samples were transported back to the University of California at Santa Barbara and analyzed within 4 h of collection. CO<sub>2</sub> concentrations were measured using a gas chromatograph (Shimadzu Model 14) equipped with a thermal conductivity detector.

## Modeling of Soil CO<sub>2</sub> Production Rates

We used the method described in Davidson and Trumbore (1995) to predict monthly average CO<sub>2</sub> production rates through each soil profile. The method is based on Fick's law of diffusion: The diffusive flux rate of a gas in soil is proportional to its concentration gradient. To be more specific, the steady-state flux of CO<sub>2</sub> from any point in the soil profile ( $F$ ) is a function of the CO<sub>2</sub> concentration gradient ( $dC$ ) with soil depth ( $dZ$ ) multiplied by a diffusion coefficient for CO<sub>2</sub> through soil ( $D_s$ ). Mathematically this is

$$F = D_s \times \frac{dC}{dZ} \quad (1)$$

A major source of uncertainty in the calculation of CO<sub>2</sub> production rates using Eq. 1 is the accuracy of  $D_s$  for individual soil layers (Thorstenson and Pollock 1989; Amundson and Davidson 1990; Pumpanen and others 2003). We used the model described by Millington and Shearer (1971) to estimate values for  $D_s$  in each soil horizon over the study period. The model has been previously applied to soil and should provide robust estimates of  $D_s$  across the spatially and temporally heterogeneous environment of the study site (Collin and Rasmuson 1988; Davidson and Trumbore 1995). Conceptually, the model assumes that all movement of CO<sub>2</sub> through the soil profile occurs through air-filled pore spaces (the diffusion of gases through water being many times slower than through air), with the model dividing soil pore spaces into either inter- or intra-aggregate pore spaces. The model is as follows:

$$D_s = D_o \left\{ \left[ \frac{\left(\frac{a_{ra}}{\varepsilon_{ra}}\right)^2 \left(\frac{a_{ra}}{\varepsilon_{ra}+S}\right)^{2x} (1 - \varepsilon_{er}^{2y}) (a_{er} - a_{er}^{2z})}{\left(\frac{a_{ra}}{\varepsilon_{ra}}\right)^2 \left(\frac{a_{ra}}{\varepsilon_{ra}+S}\right)^{2x} (1 - \varepsilon_{er}^{2y}) + (a_{er} - a_{er}^{2z})} \right] + \left[ a_{er}^{2z} \left(\frac{a_{er}}{\varepsilon_{er}}\right)^2 \right] \right\} \quad (2)$$

where  $\varepsilon_{ra}$  and  $\varepsilon_{er}$  describe total intra- and inter-aggregate pore space (in cm<sup>3</sup> pore space cm<sup>-3</sup> bed

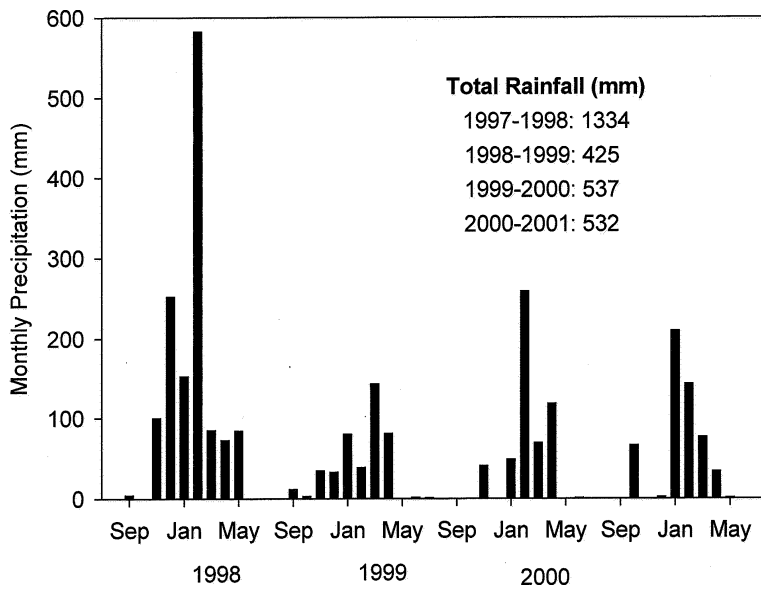


**Figure 2.** Monthly rainfall at the field site over the course of the study period (September 1997–June 2001). Total rainfall amounts were summed over the hydrologic year, defined here as September to August (with the exception of 2000–2001, when records stopped in June 2001). All data are from the Cachuma Lake NOAA weather station.

space), respectively. Air-filled intra-aggregate and interaggregate pore space (in  $\text{cm}^3$  air  $\text{cm}^{-3}$  bed space) are described by  $a_{ra}$  and  $a_{er}$ , respectively.  $D_o$  is the diffusion coefficient for CO<sub>2</sub> through air at the soil temperature measured with the installed thermocouples ( $0.162 \text{ cm}^2 \text{ s}^{-1}$  for soil at  $25^\circ\text{C}$ ).  $S$  is the space occupied by solids ( $\text{cm}^3$  solids  $\text{cm}^{-3}$  bed space). The following equations were used to calculate  $x$ ,  $y$ , and  $z$ :

$$\left(\frac{a_{ra}}{\varepsilon_{ra} + S}\right)^{2x} + \left(1 - \frac{a_{ra}}{\varepsilon_{ra} + S}\right)^x = 1 \quad (3)$$

$$\varepsilon_{er}^{2y} + (1 - \varepsilon_{er})^y = 1 \quad (4)$$

$$a_{er}^{2z} + (1 - a_{er})^z = 1 \quad (5)$$

Total porosity ( $\varepsilon$ ) for each sampled horizon was calculated from the measured bulk density values (Table 1), assuming a particle density of  $2.65 \text{ g cm}^{-3}$  (Shipman 1972). By definition, intra-aggregate pore spaces are entirely water-filled at soil field capacity and interaggregate pore spaces are water-filled only when soil water contents exceed field capacity (Millington and Shearer 1971). Therefore, interaggregate porosity can be estimated as the difference between total porosity ( $\varepsilon$ ) and the volumetric water content at field capacity ( $\theta_{fc}$ ), with intra-aggregate porosity equal to  $\theta_{fc}$  (Davidson and Trumbore 1995). To use this approach to calculate inter- and intra-aggregate porosity, we must obtain accurate in situ estimations of  $\theta_{fc}$  for each of the soil horizons in the studied profiles. Because field

capacity can be defined as the water content after a saturated soil has drained freely (Hillel 1998), we used an approach similar to that used by Davidson and Trumbore (1995) and estimated in situ values for  $\theta_{fc}$  using water content data collected from all the profiles in the last week of February 1998. The data were collected 48 h after the last of a number of large rain events (totalling  $>50 \text{ cm}$  of precipitation) that brought all the soil profiles close to saturation (Chamran and others 2002). With the exception of soil water contents measured within 24 h of large rainfall events (when soil water contents in surface horizons are likely to have exceeded  $\theta_{fc}$ ), the estimated values of  $\theta_{fc}$  represent the maximum water content observed in individual soil horizons over the course of the study period. Errors in the estimation of  $\theta_{fc}$  for individual soil horizons are not likely to have a large influence on CO<sub>2</sub> production estimates; changing  $\theta_{fc}$  values by  $\pm 20\%$  changed the final estimates of net CO<sub>2</sub> production for each soil profile by  $\pm 5\%$ .

The first term of Eq. 2 describes diffusion within the intra-aggregate air space, while the second term describes diffusion within the interaggregate pore space. It is assumed that intra-aggregate spaces fill with water first and lose water last. When volumetric soil water contents ( $\theta$ ) at any point in time are less than or equal to  $\varepsilon_{ra}$ ,  $\varepsilon_{er}$  is entirely air-filled and  $a_{er} = \varepsilon_{er}$ , so  $a_{ra}$  equals  $\varepsilon_{ra} - \theta$ . When water contents are greater than  $\varepsilon_{ra}$ ,  $a_{ra} = 0$ , so we assume that  $a_{er}$  equals  $\varepsilon - \theta$ .

CO<sub>2</sub> production rates within each profile were modeled using monthly average values for  $D_s$  and the monthly average CO<sub>2</sub> concentrations in each identifiable soil horizon. Although the CO<sub>2</sub> and

soil water content data were collected from the profiles at more frequent intervals than once a month, we decided to use monthly averages to reduce error associated with individual measurements. By using monthly averages, we lose the ability to discern the short-term dynamics of soil CO<sub>2</sub> production following individual rainfall events but we gain more robust estimations of the interannual variability in soil CO<sub>2</sub> production across the six distinct profiles.

Measured soil air CO<sub>2</sub> concentrations and estimated  $D_s$  values through each profile were linearly interpolated between sampling points at 20-cm increments using Matlab (Version 6.1, Mathworks Inc.), with the soil surface and the deepest CO<sub>2</sub> probe providing the upper and lower boundaries for each profile. CO<sub>2</sub> production rates for each 20-cm interval ( $F_i$  in mg C–CO<sub>2</sub> m<sup>-2</sup> h<sup>-1</sup>) were then calculated for the top and bottom of each depth interval using a modification of Fick's first law:

$$F_i = [D_{s,i} \times (C_i - C_{i-1})/z] - [D_{s,i+1} \times (C_{i+1} - C_i)/z] \quad (6)$$

where  $D_{s,i}$  and  $D_{s,i+1}$  are the interpolated values of  $D_s$  (in m<sup>2</sup> h<sup>-1</sup>) calculated from Eq. 2 for the 20-cm-depth interval ( $i$ ) and the 20-cm-depth interval immediately below ( $i+1$ ).  $C_{i-1}$  and  $C_{i+1}$  represent the interpolated concentrations of CO<sub>2</sub> (mg C–CO<sub>2</sub> m<sup>-3</sup>) in soil air in the 20-cm-depth interval above and below the chosen interval  $i$ , respectively.  $z$  is the depth interval (0.2 m). Some of the basic assumptions of the model are as follows: There is no downward flux of CO<sub>2</sub> at the deepest depth interval, gaseous diffusion is the only mechanism of CO<sub>2</sub> transport (no convective transport), the flux of CO<sub>2</sub> is independent of the concentration of other soil gases, and the soil atmosphere is in isobaric equilibrium with the surface atmosphere. The model also assumes that CO<sub>2</sub> concentrations are in steady state, a reasonable assumption given that Eq. 6 uses monthly average values for  $C$  and  $D_s$ .

The interpolation of  $D_s$  and CO<sub>2</sub> concentration data by 20-cm-depth intervals through the profile may introduce error in the estimations of CO<sub>2</sub> production for each particular interval ( $F_i$ ), but the relative estimates of CO<sub>2</sub> production for larger depth increments should be reasonably accurate (Davidson and Trumbore 1995). CO<sub>2</sub> production estimates for larger depth increments are calculated by summing the production estimates for the individual depth intervals. Net CO<sub>2</sub> production for the entire soil profile is calculated by summing the production estimates for all depth intervals, from the soil surface to the deepest depth interval.

## Soil Radon Activity Depth Profiles

We measured <sup>222</sup>Rn activities in the soil air of Profiles 10 and 19 in January 2000, May 2001, and June 2001. <sup>222</sup>Rn measurements were made by direct alpha counting of 50-mL soil air samples collected from the installed gas sampling probes. Radon activities of the air samples were determined using the methods described in Davidson and Trumbore (1995). Briefly, air samples were dried and alpha emissions were detected by scintillation counting using a Pylon <sup>222</sup>Rn detector (Model AB-5, Pylon Electronics, Inc., Ottawa, Canada). All cells were counted within 24 h of sample collection. Radon content was determined from the count rate after subtracting a cell blank (0.7–0.9 counts min<sup>-1</sup>) and correcting for cell efficiency (Davidson and Trumbore 1995).

Soil <sup>222</sup>Rn production rates were measured in the laboratory with one soil sample collected from each of the seven soil horizons of Profile 19 (as indicated in Table 1) in April 1997. Soil samples (10 g dry wt equivalent) were kept at field moisture levels and sealed in gas-tight 0.25-L jars. After a 14-d incubation period, during which <sup>222</sup>Rn should come to secular equilibrium with the <sup>226</sup>Ra parent, the <sup>222</sup>Rn activity of the headspace air was determined using the methods described above. <sup>222</sup>Rn production rates were calculated as the change in headspace <sup>222</sup>Rn activity over the 14-d incubation.

To test the accuracy of the estimated soil gas diffusivity constants ( $D_s$  in Eqs. 2 and 6), we compared measured and predicted soil air <sup>222</sup>Rn activities. A similar approach has been applied to other studies of gaseous diffusion through soil (Dorr and Munnich 1990; Davidson and Trumbore 1995). We predicted steady-state soil air <sup>222</sup>Rn concentrations as a function of soil depth using an equation adapted from Dorr and Munnich (1990):

$$[^{222}\text{Rn}]_z = [^{222}\text{Rn}]_\infty \left(1 - e^{-z\sqrt{(\lambda/D_s)}}\right) \quad (7)$$

where  $[^{222}\text{Rn}]_z$  is <sup>222</sup>Rn concentration in soil air (in kBq m<sup>-3</sup> air) at depth  $z$  (in cm),  $\lambda$  is the decay constant for <sup>222</sup>Rn ( $2.1 \times 10^{-6}$  s<sup>-1</sup>),  $D_s$  the effective diffusivity of <sup>222</sup>Rn in soil (in cm<sup>2</sup> s<sup>-1</sup>) at depth  $z$ , and  $[^{222}\text{Rn}]_\infty$  is the <sup>222</sup>Rn concentration at an infinite depth. We assume that when the <sup>222</sup>Rn concentrations in soil air approach the value for  $[^{222}\text{Rn}]_\infty$ , a steady state between <sup>222</sup>Rn production and decay is reached and any diffusional losses of <sup>222</sup>Rn can be ignored.  $D_s$  and  $[^{222}\text{Rn}]_\infty$  values were calculated for each gas sampling depth within each profile at each of the three sampling times so we could directly compare predicted and measured

values of [<sup>222</sup>Rn].  $D_s$  was calculated using Eq. 2 with a  $D_o$  of 0.135 cm<sup>2</sup> s<sup>-1</sup>, the diffusion coefficient for <sup>222</sup>Rn in air at 25°C. [<sup>222</sup>Rn]<sub>∞</sub> was calculated using

$$[^{222}\text{Rn}]_{\infty} = P \times \rho_b \times \frac{1}{a + 0.22w} \quad (8)$$

where  $P_i$  is <sup>222</sup>Rn production in kBq kg<sup>-1</sup> soil, as determined from the laboratory incubations,  $\rho_b$  is soil bulk density in kg in<sup>-3</sup>,  $a$  is air-filled pore space (m<sup>3</sup> air m<sup>-3</sup> bed space),  $w$  is water-filled pore space (m<sup>3</sup> H<sub>2</sub>O m<sup>-3</sup> bed space), and 0.22 is the partition coefficient for <sup>222</sup>Rn between water and gas phases at 25°C (Nazaroff 1992).

### Surface CO<sub>2</sub> Flux Measurements

Vented, dynamic chambers (15.5 L in volume) were placed on collars preinstalled to 5-cm depth in the soil surface at fixed locations within 1 m of each of the six instrumented profiles. Care was taken to minimize disturbance to the existing vegetation when placing the collars in the soil. CO<sub>2</sub> fluxes in each chamber were measured with an infrared gas analyzer (Model LI-800, LI-COR Inc., Lincoln, NE). CO<sub>2</sub> fluxes were measured weekly between January and July 2001. At each sampling time, one measurement was taken at each profile using a 5-s averaging of CO<sub>2</sub> concentrations within each chamber for a period of no less than 90 s. The CO<sub>2</sub> flux across the soil-air interface (in mg CO<sub>2</sub> m<sup>-2</sup> h<sup>-1</sup>) was then calculated using the methods described in Khalil and others (1998). Surface CO<sub>2</sub> fluxes from each profile were measured within 2 h of one another, usually around midday. Additional details on the measurement of surface CO<sub>2</sub> fluxes at the profiles can be found in Hooper (2003).

### <sup>14</sup>C Analysis of CO<sub>2</sub> and Soil Organic C

CO<sub>2</sub> in gas samples and CO<sub>2</sub> emitted from the soil surface were collected from Profiles 10 and 19 at one time point (in January 2000) and analyzed for <sup>14</sup>C content at the Center for Accelerator Mass Spectrometry at Lawrence Livermore Laboratory (Livermore, California) using methods detailed in Gaudinski and others (2000). Gas samples from the soil profiles were collected by attaching pre-evacuated stainless-steel canisters to the sampling probes, using a capillary restriction to ensure that they filled over a period of several hours. CO<sub>2</sub> emitted from the soil surface was collected by passing air from a dynamic chamber through soda lime (to remove any ambient air CO<sub>2</sub>) and through a molecular sieve 13X trap, as detailed in Gaudinski and others (2000). CO<sub>2</sub> was purified cryogenically

from the air in the canisters and reduced to graphite using a method of Zn reduction modified from Vogel (1992).

Soil samples were collected from each horizon of Profiles 10 and 19 in April 1997. Samples from the uppermost horizons were separated using sodium polytungstate into low (<2 g cm<sup>-3</sup>) and high density (>2 g cm<sup>-3</sup>) fractions (Gaudinski and others 2000). Soils were combusted under vacuum at 900°C with cupric oxide wire and the resulting CO<sub>2</sub> was cryogenically purified and reduced to graphite for <sup>14</sup>C analysis.

The <sup>14</sup>C composition of soil organic C and CO<sub>2</sub> is expressed in  $\Delta^{14}\text{C}$  values, the per mil deviation from the <sup>14</sup>C:<sup>12</sup>C ratio of an oxalic acid standard in 1950. Radiocarbon samples are corrected to a common <sup>13</sup>C value of -25‰ to adjust for mass-dependent isotopic fractionation. Details on the calculation  $\Delta^{14}\text{C}$  can be found in Stuiver and Polach (1977).

## RESULTS AND DISCUSSION

### Soil Water Dynamics

Rainfall varied considerably over the course of the study period (Figure 2). Such a high degree of temporal variability in rainfall is typical of the climate in coastal southern California (Rambal and Debussche 1995). A strong El Niño event occurred during the winter of 1997–1998, producing one of wettest years on record for the study area and bringing the soil profiles to some of the highest soil moisture levels we measured over the course of the study period (Figure 3). In contrast, the La Niña year of 1998–1999 was a below-average rainfall year (Figure 2) and soil moisture levels were relatively low (Figure 3). Although the 1999–2000 and 2000–2001 rainfall years had similar total amounts of precipitation (Figure 2), the soil profiles had slightly higher moisture levels in 2000–2001 (Figure 3). Individual rain events were smaller in magnitude in the winter of 2001 than in 2000 (data not shown), so the higher soil moisture levels observed in 2001 are likely a result of higher average infiltration rates.

### Soil CO<sub>2</sub> Concentrations

Soil air CO<sub>2</sub> concentrations generally increased with profile depth (Figure 4), a common observation in many soils (Amundson and Davidson 1990). High levels of inter- and intra-annual variability in soil CO<sub>2</sub> concentrations were observed in all six profiles. In general, CO<sub>2</sub> concentrations were positively related to soil water contents. Profile CO<sub>2</sub>

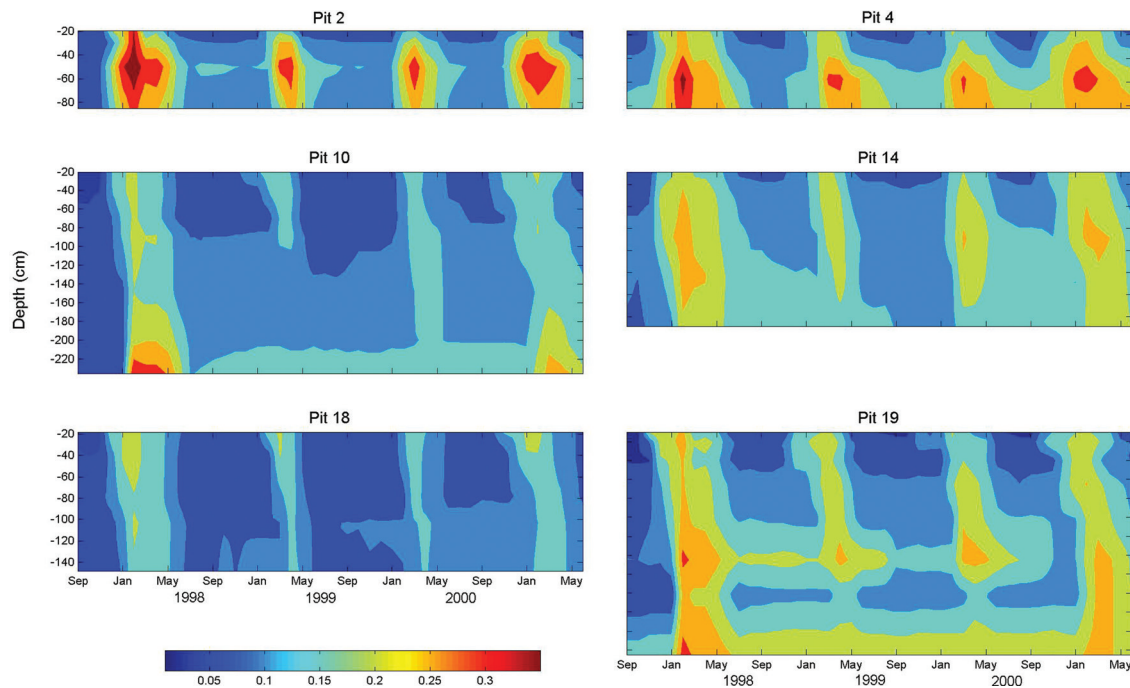


**Figure 3.** Volumetric soil water contents (in cm<sup>3</sup> H<sub>2</sub>O cm<sup>-3</sup> soil) within all six profiles over the course of the study period. All six images use the same color scale to emphasize relative differences in soil water contents between profiles. The y axis are scaled according to profile depth.

concentrations were highest during the El Niño winter of 1997–1998 when measured CO<sub>2</sub> concentrations exceeded 20 mmol CO<sub>2</sub> mol<sup>-1</sup> air in the deeper soil horizons (Figure 4). The seasonal trend in profile CO<sub>2</sub> concentrations is very distinct; profile CO<sub>2</sub> concentrations were always much higher in the wet winter months than in the dry summer months (Figure 4). A similar annual pattern in profile CO<sub>2</sub> concentrations has been observed in other semiarid and grassland soils (Wood and Pe-traitis 1984; Amundson and Davidson 1990). An increase in soil water contents should raise soil air CO<sub>2</sub> concentrations by simultaneously reducing the diffusion of CO<sub>2</sub> through the profile and increasing the rates of biotic CO<sub>2</sub> production.

### Radon Activity Profiles

Soil <sup>222</sup>Rn production rates ( $P_i$  in Eq. 8) deviated by less than 10% throughout Profile 19, averaging 0.01 kBq kg<sup>-1</sup> dry soil. This rate is within the range of <sup>222</sup>Rn production rates reported for other soils (Nazaroff 1992). We assumed that <sup>222</sup>Rn production rates do not differ significantly between Profiles 10 and 19 and used the same value of  $P_i$  for the calculation of [<sup>222</sup>Rn]<sub>∞</sub> (Eq. 8) in both profiles.

The close relationship between actual and predicted <sup>222</sup>Rn concentrations in soil air (Figure 5)

suggests that the diffusion model (Eq. 2) performed adequately in both profiles. However, it is worth noting that the relative differences between actual and predicted <sup>222</sup>Rn soil air concentrations were greater in Profile 10 than in Profile 19, particularly for the January 2000 and June 2001 sampling dates. The consistent overestimation of <sup>222</sup>Rn soil air concentrations is most likely associated with an overestimation of <sup>222</sup>Rn production ( $P_i$ ). We determined  $P_i$  at field moisture levels (samples were collected in April 1997) when the soil moisture levels were higher than in January 2000 or June 2001 (data not shown). Because <sup>222</sup>Rn production rates are generally lower when soils are dry, due to a decrease in the <sup>222</sup>Rn emanation coefficient (Stranden and others 1984), we have probably overestimated the in situ rates of <sup>222</sup>Rn production. Despite this, the diffusion model used in this study (Eq. 2) provided reasonably accurate estimates of gaseous diffusion rates through soil profiles at the study site.

### Measured Versus Modeled Net Fluxes of CO<sub>2</sub> to the Atmosphere

Over a six-month period in 2001, surface CO<sub>2</sub> fluxes were measured in close proximity to each of the six profiles. In general, the measured rate of

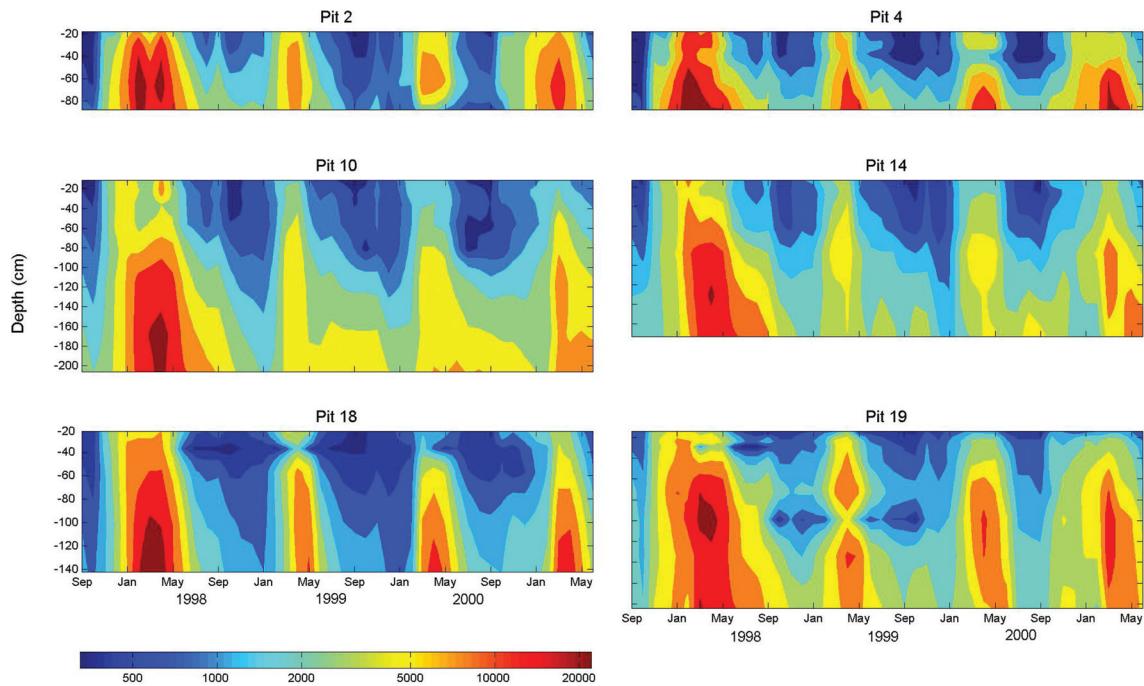


Figure 4. Soil air CO<sub>2</sub> concentrations (in  $\mu\text{mol CO}_2 \text{ mol}^{-1} \text{ air}$ ) within the soil profiles over the course of the study period. The color bar is logarithmic. The y axis are scaled according to profile depth.

CO<sub>2</sub> emission at the soil surface peaked between February and March (Figure 6), the height of the plant-growing season. After plant senescence in late April, CO<sub>2</sub> fluxes decreased significantly. Profile 4 had the highest CO<sub>2</sub> emission rate during the wet season with measured fluxes in February exceeding  $140 \text{ mg C-CO}_2 \text{ m}^{-2} \text{ h}^{-1}$ . In the other five profiles, peak rates ranged from 70 to  $100 \text{ mg C-CO}_2 \text{ m}^{-2} \text{ h}^{-1}$ . Net rates were generally 2–10 times lower in the relatively dry months of May and June than in the wetter months of January to April (Figure 6).

If we compare the measured surface CO<sub>2</sub> fluxes to the net profile fluxes estimated from Eq. 6, we can ascertain how well our model predicted surface CO<sub>2</sub> fluxes from each profile (Figure 6). The modeled and measured surface CO<sub>2</sub> fluxes were very similar when the soils were relatively dry (April to June), but the model consistently underestimated fluxes between January and March, when the profiles were relatively moist. The disparity between modeled and measured fluxes during the wet months was particularly large for Profiles 4, 10, and 19 (Figure 6).

The underestimation of net profile CO<sub>2</sub> fluxes during the wet months is not surprising since Fick's law approaches tend to underestimate CO<sub>2</sub> production in near-surface soil layers, underestimating the net flux of CO<sub>2</sub> at the soil/atmosphere interface

(Davidson and Trumbore 1995; Billings and others 1998; Elberling 2003). A Fick's law approach is best applied when the concentration gradient through the soil profile is well characterized (Thorstenson and Pollock 1989). The shallowest gas probes were installed at 10–20-cm depth and the measured CO<sub>2</sub> concentrations at these probe depths were often close to atmospheric concentrations (due to high rates of CO<sub>2</sub> transport), so we were not able to accurately estimate the CO<sub>2</sub> concentration gradients in the near-surface soil horizons. In addition, our model assumes that all transport of CO<sub>2</sub> through the profile is by molecular diffusion. This assumption is probably reasonable for the deeper soil horizons (Wood and Petraitis 1984), but in the near-surface horizons there is likely to be considerable convective transport of CO<sub>2</sub> through soil macropores, especially at the times of the year when the soil is dry. Our underestimation of CO<sub>2</sub> production in near-surface soil horizons would lead to the observed underestimation of net profile CO<sub>2</sub> production during the wet season, when rates of biotic CO<sub>2</sub> production in near-surface horizons are quite high. Our estimates of net CO<sub>2</sub> production are much more accurate when the uppermost soil horizons are dry and biotic CO<sub>2</sub> production in the near-surface soil horizons is diminished.

There are a number of possible explanations for the poor correlation between predicted and mea-

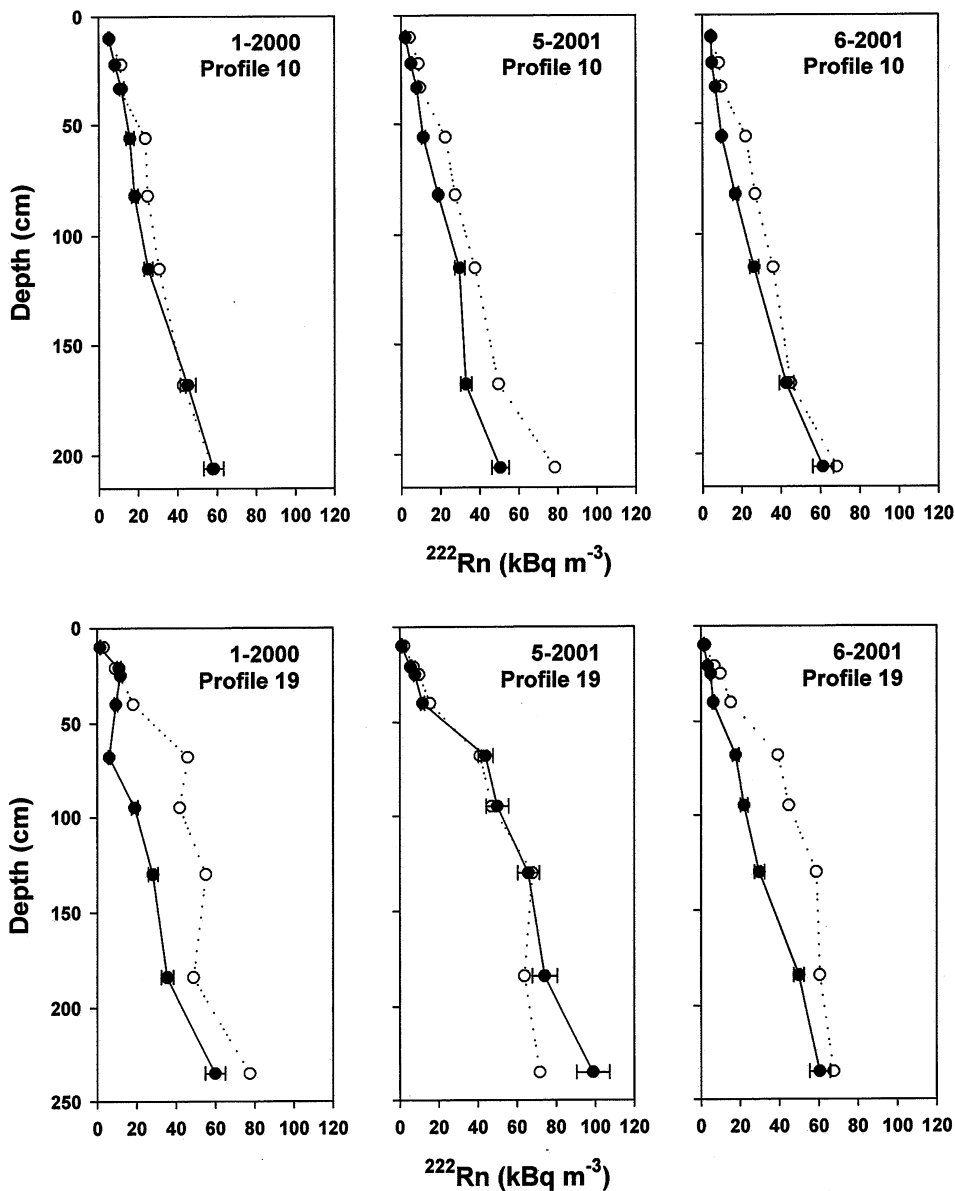


Figure 5. Modeled and measured  $^{222}\text{Rn}$  activities through Profiles 10 and 19 at three time points. Unfilled circles with dashed lines represent modeled  $^{222}\text{Rn}$  activities and the filled circles with solid lines represent the measured  $^{222}\text{Rn}$  activities in soil gas samples collected from the profiles. Error bars represent analytical uncertainty in the measurement of  $^{222}\text{Rn}$  activity.

sured surface  $\text{CO}_2$  fluxes from Profile 4. If  $\text{CO}_2$  production in the near-surface horizons was significantly higher in Profile 4 than in the other five profiles, the magnitude of the error associated with the underestimation of  $\text{CO}_2$  production in near-surface horizons (see above) would be greater for Profile 4. This explanation is not likely; the organic C contents and aboveground net productivity measured at Profile 4 are near-average for all of the studied profiles (Table 1), so we would not expect Profile 4 to have unusually high rates of  $\text{CO}_2$  production in the near-surface horizons. However, the surface flux chamber for Profile 4 may have been placed above an organic-rich soil microsite with anomalously high rates of  $\text{CO}_2$  production near the soil surface (the chamber

locations were unchanged over the six-month measurement period). Alternatively, the observed disparity between the measured and modeled  $\text{CO}_2$  fluxes at Profile 4 may be a result of the well-developed and smectite-rich argillic horizon that is found at 30–40-cm depth in this profile but not in any of the other studied profiles (O. Chadwick personal observation). A smectite-rich horizon is likely to swell when wet, effectively blocking the diffusion of  $\text{CO}_2$  from the deeper horizons. Because our model does not take into account any changes in the rate of gaseous  $\text{CO}_2$  diffusion that would result from the expansion of this smectite-rich horizon, we may have significantly overestimated  $\text{CO}_2$  transport into or out of the deeper soil horizons of Profile 4.

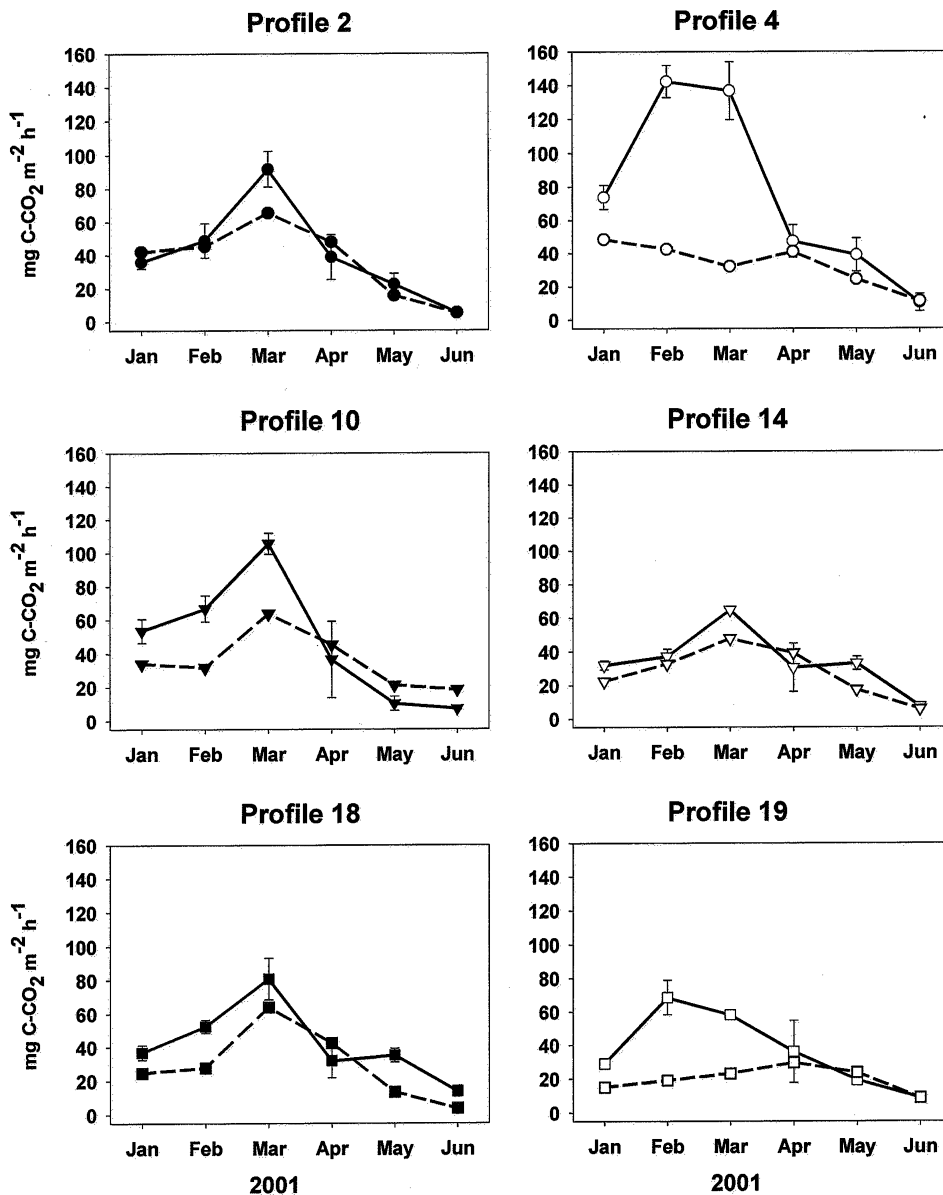


Figure 6. Modeled net rates of CO<sub>2</sub> production (dashed lines) versus measured rates of CO<sub>2</sub> production (solid lines) for each profile. Measured rates were determined weekly using surface flux chambers placed within 1 m of each instrumented profile. Error bars indicate  $\pm 1$  standard error of the monthly mean value.

Overall, the model we used to estimate soil CO<sub>2</sub> production rates performed reasonably well. This statement is supported by two lines of evidence: (1) Radon activity profiles show that our estimates of  $D_s$ , the largest source of uncertainty in any model of gas movement through soil, can be used to accurately predict soil air <sup>222</sup>Rn concentrations (Figure 5). (2) If we exclude Profile 4, the modeled estimate for hillslope CO<sub>2</sub> flux from January to July 2001 is, on average, only 10%–20% lower than the measured estimate of hillslope CO<sub>2</sub> flux (Figure 6). Although the model has some clear limitations, namely, the inability to accurately estimate CO<sub>2</sub> production in the near-surface soil horizons, this study and other studies have observed a good correlation between net CO<sub>2</sub> fluxes modeled using

Fick's law-based approaches and CO<sub>2</sub> fluxes measured with surface chambers (Davidson and Trumbore 1995; Yavitt and others 1995; Yoshikawa and Hasegawa 2000). At the very least, we can use the model to better understand how production in deeper soil horizons is affected by environmental conditions.

### Modeled Soil CO<sub>2</sub> Production Across Time

Figure 7 shows modeled net CO<sub>2</sub> production per month over the three-year study period for five of the six profiles (Profile 4 was excluded because of the large disparity between modeled and measured CO<sub>2</sub> fluxes at the soil surface). There is a pro-

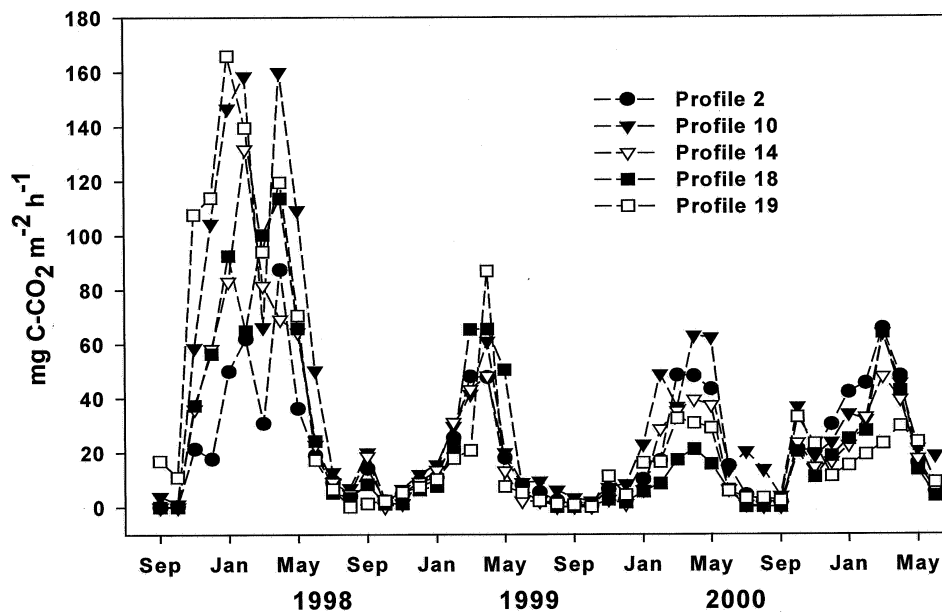


Figure 7. Modeled net rates of  $\text{CO}_2$  production for each profile (in  $\text{mg C-CO}_2 \text{ m}^{-2} \text{ h}^{-1}$ ) over the course of the study period. Rates were estimated using Eq. 6. Profile 4 has been excluded.

nounced annual cycle in soil  $\text{CO}_2$  production; the average net rate of  $\text{CO}_2$  production for the five profiles over the wet season (December to May) was generally 2.5–10 times higher than the average rate during the dry season (June to November) of the same year (Table 2). Considering that our model underestimated  $\text{CO}_2$  production in near-surface horizons (see above), the differences between wet season and dry season soil  $\text{CO}_2$  production are likely to be even greater in magnitude. With the exception of the El Niño year, when  $\text{CO}_2$  production rates fluctuated significantly over the course of the wet season but remained high from December to May,  $\text{CO}_2$  production rates peaked over a relatively short time period, generally between March and April (Figure 7). The annual pattern in soil  $\text{CO}_2$  flux suggests that  $\text{CO}_2$  production in this system is most strongly influenced by plant phenology and soil water content, a common observation in other semiarid ecosystems (Rovira and Vallejo 1997; Hendry and others 1999). We would expect high rates of both autotrophic and heterotrophic respiration during the wet months of the year when soil moisture levels are closer to optimal for microbial respiration and the annual grasses are actively growing, respiring  $\text{CO}_2$  and supplying labile organic C to soil microorganisms. Work conducted at the study site by Hooper (2003) suggests that plant-dependent  $\text{CO}_2$  production (either root respiration or the microbial mineralization of root exudates) accounts for 60%–80% of hillslope  $\text{CO}_2$  production during the wet season. The drying of the soils (Figure 3) and the onset of plant senescence in early summer coincide with the

sharp decline in soil  $\text{CO}_2$  production in June (Figure 7). Although a positive relationship between soil temperature and biotic  $\text{CO}_2$  production is commonly observed in soils (Raich and Schlesinger 1992; Schimel and others 1994), temperature does not seem to be a particularly important control on the rates of  $\text{CO}_2$  production at this semiarid grassland site. Over the study period, the average air temperature during the dry season ( $27^\circ\text{C}$ ) was much higher than the average wet season air temperature ( $19^\circ\text{C}$ ). This pattern is reflected in the soil temperatures measured between 10 and 25 cm in the studied profiles, which averaged  $24^\circ\text{C}$  and  $14^\circ\text{C}$  for the dry and wet seasons, respectively. Because the surface soil horizons at the study site are typically very dry during the warm summer months (Figure 3), soil moisture has a larger influence on the rates of biotic  $\text{CO}_2$  production than soil temperature.

There was also a high degree of interannual variability in profile  $\text{CO}_2$  production, particularly if we compare the El Niño year of 1997–1998 with the succeeding non El Niño years (Figure 7). The average respiration rate for all five profiles was approximately three times higher during the 1997–1998 wet season than in the other three wet seasons (Table 2). The high soil moisture levels observed during the El Niño year (Figure 3) result in higher and more sustained rates of biotic  $\text{CO}_2$  production than in the non-El Niño years. Although the total amount of precipitation for the La Niña year of 1998–1999 was slightly lower than the recorded precipitation for the 1999–2000 and 2000–2001 rainfall years (Figure 2), the average

**Table 2.** Modeled Net Rates of CO<sub>2</sub> Production and the Contribution of the Subsurface Horizons to the Net Flux of CO<sub>2</sub> from the Soil Profiles

Season	Modeled net rates of CO <sub>2</sub> production (mg C-CO <sub>2</sub> m <sup>-2</sup> h <sup>-1</sup> )		Subsurface contribution to whole profile CO <sub>2</sub> production (% of total)
	Whole profile	Subsurface layer	
Wet 1997–1998	90.5 (7.2)	28.9 (5.1)	31.9 (6.6)
Dry 1998	9.9 (2.1)	4.1 (1.0)	41.3 (14.7)
Wet 1998–1999	28.8 (4.0)	9.6 (2.4)	33.3 (8.9)
Dry 1999	4.5 (1.1)	2.6 (0.7)	56.6 (12.8)
Wet 1999–2000	25.1 (3.3)	8.7 (2.0)	34.5 (15.7)
Dry 2000	10.8 (1.9)	2.2 (0.7)	20.3 (6.9)
Wet 2000–2001	31.8 (2.8)	10.8 (2.3)	34.0 (12.7)

Subsurface soil layers = all horizons below 40 cm in depth. Wet season = December to May. Dry season = June to November. Production rates represent the mean rates per season for all five of the six studied profiles combined. Profile 4 was excluded because the model did not perform adequately (see text). One standard error of the mean indicated in parentheses. Whole profile CO<sub>2</sub> production rates for the wet seasons are likely to be underestimates because CO<sub>2</sub> production rates in near-surface soil horizons could not be quantified accurately (see text).

rates of CO<sub>2</sub> production during the three wet seasons following the El Niño event were not considerably different. In years of near-average rainfall, intra-annual patterns in rainfall distribution may have a larger effect on net soil CO<sub>2</sub> production than total annual rainfall amounts.

### Surface Versus Subsurface Production of CO<sub>2</sub>

Using the Fick's law approach, we can estimate net profile CO<sub>2</sub> production (as in Figure 7) and the rates of CO<sub>2</sub> production in individual layers of the soil profile. For the sake of simplicity, we divide each profile into surface (0–40-cm-depth interval) and subsurface layers (soil below 40 cm in depth). By dividing the profiles in this manner, we can estimate the relative contribution of CO<sub>2</sub> production in deeper soil horizons to net profile CO<sub>2</sub> fluxes. Although this surface-versus-subsurface designation is somewhat arbitrary, the boundary between A and B horizons (or A and AB horizons) is generally around 40 cm deep at the study site (Table 1) and the plant rooting zones are limited to the top 40 cm of the soil profiles (O. Chadwick personal observation).

During the wet seasons, the subsurface layers contribute to approximately 30% of whole profile CO<sub>2</sub> production (Table 2). Because our model underestimates near-surface CO<sub>2</sub> production during the wet season (see above and Figure 6), the actual contribution of subsurface layers to net profile CO<sub>2</sub> production is likely to be lower than estimated. During the dry seasons, CO<sub>2</sub> production in subsurface layers is 20%–56% of whole-profile CO<sub>2</sub> production (Table 2). The modeled and mea-

sured net rates of CO<sub>2</sub> flux are very similar during dry months (Figure 6), so the dry season estimates of the subsurface contribution to whole-profile CO<sub>2</sub> production should be reasonably accurate. The estimated contribution of the subsurface layers to whole-profile CO<sub>2</sub> production was lowest in the dry season of 2000 (20%, Table 2); this is most likely the result of a pulse in surface-layer CO<sub>2</sub> production that occurred in October 2000 following a “dry season” rain event (Figure 2).

During the wet seasons, the rates of CO<sub>2</sub> production in the surface soil layers are considerably higher than the rates in the subsurface layers, a pattern typical of many soils (deJong and Schappert 1972; Davidson and Trumbore 1995; Keller and Bacon 1998; Gaudinski and others 2000; Elberling 2003). We would expect the abundance of organic matter, available water, and plant roots to yield high rates of autotrophic and heterotrophic respiration in surface layers during the wet season. During the dry season, CO<sub>2</sub> production rates throughout the profile are much lower and subsurface layers play a more important role in whole-profile CO<sub>2</sub> production. The uppermost soil horizons are generally very dry and the annual grasses have senesced, severely reducing the rates of biotic CO<sub>2</sub> production in surface layers. In contrast, subsurface layers retain higher levels of soil moisture throughout the dry season (Figure 3), sustaining low, but measurable, rates of biotic CO<sub>2</sub> production. A similar annual pattern in surface-versus-subsurface CO<sub>2</sub> production has been observed in other semiarid ecosystems (Wood and Petraitis 1984; Wood and others 1993; Keller and Bacon 1998; Hendry and others 1999). We expect that the observed an-

**Table 3.**  $\Delta^{14}\text{C}$  of Belowground Soil Organic Carbon (SOC) and  $\text{CO}_2$  in Profiles 10 and 19

	Soil Organic C		Soil $\text{CO}_2$	
	Sampling Depth (cm)	$\Delta^{14}\text{C}(\text{‰})$	Sampling Depth (cm)	$\delta^{14}\text{C}(\text{‰})$
<b>Profile 10</b>	3 (low-density SOC)	44.57	aboveground atmosphere	72.90
	3 (high-density SOC)	122.12		
	18 (low-density SOC)	-32.67	soil surface	97.00
	18 (high-density SOC)	20.52		
	42	-168.04		
	66	-255.71	56	113.32
	96	-323.43		
	138	-430.47		
	184	-486.64	168	93.12
253	-557.73			
<b>Profile 19</b>	3 (low-density SOC)	119.83	aboveground atmosphere	72.90
	3 (high-density SOC)	66.97		
	15 (low-density SOC)	-24.02	soil surface	93
	15 (high-density SOC)	-65.13		
	32	-110.37	40	110.43
	60	-248.11	95	88.14
	101	-403.26	130	96.02
	140	-497.62	184	90.12
	229	-639.46	230	89.99

nual pattern in depth-specific  $\text{CO}_2$  production may be relatively common in semiarid or Mediterranean-type ecosystems that are dominated by annual plants. In ecosystems without clearly defined wet and dry seasons, less extensive subsurface horizons, or an abundance of perennial, shallow-rooted plants, the deeper soil horizons are likely to play a smaller role in net soil  $\text{CO}_2$  production.

### Sources of Subsurface $\text{CO}_2$

The  $\Delta^{14}\text{C}$  values of soil organic carbon decrease sharply with depth through the soil profiles (Table 3). A similar pattern has been observed in a number of other soil profiles (Trumbore 2000). Positive  $\Delta^{14}\text{C}$  values indicate the presence of radiocarbon produced by atmospheric nuclear weapons testing during the early 1960s. Positive values of  $\Delta^{14}\text{C}$  for soil organic C indicate that the C is "young" and dominated by C fixed within the past 30–40 years. Negative  $\Delta^{14}\text{C}$  values indicate the bulk of the C is "prebomb" and has been around for a long enough time (>300 years) for significant radioactive decay to have occurred (Trumbore 2000). The decrease in organic C  $\Delta^{14}\text{C}$  values with soil depth is evidence that the mean residence time of organic C increases significantly with soil depth. Based on the measured  $\Delta^{14}\text{C}$  values for bulk soil organic C samples collected from Profiles 10 and 19

(Table 3) and the radioactive decay constant for  $^{14}\text{C}$ , we can estimate that the mean residence times for soil organic carbon in the 0–5-cm, 30–60-cm, and 100–200-cm-depth increments are less than 40 y, 1000–2000 y, and 4000–8000 y, respectively.

Although the  $\Delta^{14}\text{C}$  values for Soil organic C decrease significantly with soil depth, the  $\Delta^{14}\text{C}$  values for soil  $\text{CO}_2$  are positive and relatively constant through the soil profile. The positive  $\Delta^{14}\text{C}$  values suggest that the bulk of the soil  $\text{CO}_2$ , even the  $\text{CO}_2$  found in the deeper soil horizons, is derived from C fixed within the past 40 years. Microbial mineralization of the "old" organic C that predominates in the deeper soil horizons cannot be a significant source of  $\text{CO}_2$  in the studied profiles. Other studies have also shown that the majority of the  $\text{CO}_2$  in soil profiles is derived from relatively "young" C sources (Davidson and Trumbore 1995; Gaudinski and others 2000).

There are four possible sources of subsurface  $\text{CO}_2$  in this system: (1) abiotic  $\text{CO}_2$  production (2) degassing of  $\text{CO}_2$  from soil water transported down the profile, (3) autotrophic respiration from plant roots, and (4) heterotrophic respiration by subsurface-dwelling soil microorganisms. By synthesizing the available information collected from the soil profiles, we can evaluate the relative importance of these four sources.

Abiotic  $\text{CO}_2$  production by carbonate dissolution is not likely to be significant at the study site:

Inorganic C concentrations are very low and carbonate dissolution would yield highly negative  $\Delta^{14}\text{C}$  values for soil CO<sub>2</sub>. Other abiotic sources of CO<sub>2</sub> (such as chemical oxidation) should be too small in magnitude to satisfy the observed fluxes (Wood and Petraitis 1984). If the rates of georespiration (*sensu* Keller and Bacon 1998) were significant in the profiles, the  $\Delta^{14}\text{C}$  values of soil CO<sub>2</sub> would be more negative.

The exsolution of CO<sub>2</sub> from surface water moving downward through the profile is not likely to account for the majority of CO<sub>2</sub> production in the deeper horizons of the profiles. If we assume that the surface layer of a soil profile (the top 40 cm, as defined above) has a mean  $\theta_{\text{fc}}$  of 0.25 cm<sup>3</sup> H<sub>2</sub>O cm<sup>-3</sup> soil at the study site, the surface 40-cm soil layer (1 m<sup>2</sup> in area) could store 100 L of H<sub>2</sub>O at field capacity. If we assume that this volume of soil water is at 20°C, with an alkalinity of 2 meq L<sup>-1</sup> and a pH of 7.0, the entire volume of soil water could hold a maximum of 240 mmol dissolved inorganic C (Stumm and Morgan 1981). If we then assume that this entire volume of soil water moves to the subsurface layer (the maximum possible hydrologic drainage across the 40-cm boundary), releasing all of the dissolved CO<sub>2</sub> as gaseous CO<sub>2</sub> over a six-month period, the CO<sub>2</sub> production rate in the subsurface layer would be on the order of 0.7 mg C–CO<sub>2</sub> m<sup>-2</sup> h<sup>-1</sup>. The estimated rates of CO<sub>2</sub> production in subsurface horizons (Table 2) are considerably greater than the maximum amount of CO<sub>2</sub> that could be produced by the exsolution of CO<sub>2</sub> transported downward in soil water. The exsolution of CO<sub>2</sub> from soil water may contribute to subsurface CO<sub>2</sub> production, but it is not likely to be the dominant source.

The  $\Delta^{14}\text{C}$  values for soil CO<sub>2</sub> suggest that the primary source of profile CO<sub>2</sub> is recently fixed organic C (photosynthate) mineralized by either autotrophic or heterotrophic respiration. No plant roots were observed below 40 cm in any of the six profiles, so subsurface CO<sub>2</sub> production at the study sites does not seem to be directly associated with plant roots. We therefore propose that the majority of the subsurface CO<sub>2</sub> is derived from the microbial mineralization of dissolved organic C transported from surface to subsurface layers by water moving down through the soil profile. Annual grasses exude large quantities of dissolved organic C during the winter and spring months when they are actively growing. This plant-derived organic C is likely to be transported down the profile in soil water and mineralized over time by the microbial populations that reside in deeper soil horizons at the study site (see Fierer and others 2003). Relatively low concentrations of dissolved organic C

should be sufficient to sustain the low rates of microbial CO<sub>2</sub> production observed in the subsurface soil horizons. Wood and others (1993) have proposed a similar mechanism for subsurface CO<sub>2</sub> production in grassland soils. Our hypothesis may partially explain the large interannual differences in CO<sub>2</sub> production rates; the above-average levels of plant productivity and soil moisture observed during the El Niño year would result in the movement of significant amounts of plant-derived C downward through the soil profiles for subsequent mineralization by subsurface dwelling microorganisms.

## Overview

Overall, our study showed that soil hydrology and soil CO<sub>2</sub> dynamics are inextricably linked. Using a Fick's law approach, we were able to use measurements of soil moisture and soil CO<sub>2</sub> concentrations to estimate the rates of CO<sub>2</sub> production in a series of soil profiles. Although our model underestimated CO<sub>2</sub> production in the near surface soil horizons, our predicted rates of profile CO<sub>2</sub> production were, on average, only 10%–20% lower than the measured rates, allowing us to qualitatively compare soil CO<sub>2</sub> dynamics across time. Soil water availability is the major driver of soil CO<sub>2</sub> dynamics, and the inter- and intra-annual variability in soil moisture levels has marked effects on CO<sub>2</sub> production in soils. The subsurface contribution to whole-profile CO<sub>2</sub> production is likely to be relatively less during the wet season (December to May), when the rates of biotic CO<sub>2</sub> production in surface soil horizons are very high. During the dry season (June to November), the surface horizons are very dry and subsurface horizons account for a significant portion of total-profile CO<sub>2</sub> production. The majority of the CO<sub>2</sub> produced in the deeper soil horizons seems to be derived from the heterotrophic mineralization of recently fixed carbon transported down the profile in solution. Little, if any, of the soil CO<sub>2</sub> appears to be derived from the mineralization of the relatively old soil organic carbon residing in deeper soil horizons.

## ACKNOWLEDGMENT

We would like to thank Faraneh Chamran, Barry Hooper, Lynne Dee Althouse, Carrie Masiello, Karen Holmes, and Paul Gessler for their considerable assistance with this project. We would also like to thank Dan Richter for his thorough and thoughtful review of the manuscript.

## REFERENCES

- Ajwa HA, Rice CW, Sotomayor D. 1998. Carbon and nitrogen mineralization in tallgrass prairie and agricultural soil profiles. *Soil Sci Soc Am J* 62:942–51.
- Amundson R, Davidson E. 1990. Carbon dioxide and nitrogenous gases in the soil atmosphere. *J Geochem Explor* 38:13–41.
- Amundson R, Stern L, Baisden T, Wang Y. 1998. The isotopic composition of soil and soil-respired CO<sub>2</sub>. *Geoderma* 82:83–114.
- Andrews JA, Schlesinger WH. 2001. Soil CO<sub>2</sub> dynamics, acidification, and chemical weathering in a temperate forest with experimental CO<sub>2</sub> enrichment. *Global Biogeochem Cycles* 15:149–62.
- Batjes NH. 1996. Total carbon and nitrogen in the soils of the world. *Eur J Soil Sci* 47:151–63.
- Billings W. 1995. What we need to know: Some priorities for research on biotic feedbacks in a changing biosphere. In: Woodwell G, MacKenzie F, eds. *Biotic feedbacks in the global climatic system: will warming feed the warming?* New York: Oxford University Press. p 377–392.
- Billings SA, Richter DD, Yarie J. 1998. Soil carbon dioxide fluxes and profile concentrations in two boreal forests. *Can J For Res* 28:1773–83.
- Burton DL, Beauchamp EG. 1994. Profile nitrous oxide and carbon dioxide concentrations in a soil subject to freezing. *Soil Sci Soc Am J* 58:115–22.
- Cerling T, Solomon D, Quade J, Bowman J. 1991. On the isotopic composition of carbon in soil carbon dioxide. *Geochim Cosmochim Acta* 55:3404–5.
- Chamran F, Gessler P, Chadwick O. 2002. Spatially explicit treatment of soil–water dynamics along a semiarid catena. *Soil Sci Soc Am J* 66:1571–83.
- Chapin F, Matson P, Mooney H. 2002. *Principles of Terrestrial Ecosystem Ecology* New York: Springer.
- Collin M, Rasmuson A. 1988. A comparison of gas diffusivity models for unsaturated porous media. *Soil Sci Soc Am J* 52:1559–65.
- Davidson EA, Trumbore SE. 1995. Gas diffusivity and production of CO<sub>2</sub> in deep soils of the eastern Amazon. *Tellus Ser B Chem Phys Meteorol* 47:550–65.
- deJong E, Schappert H. 1972. Calculation of soil respiration and activity from CO<sub>2</sub> profiles in the soil. *Soil Sci* 113:328–33.
- Dibblee T. 1966. *Santa Ynez Mountains: Geology of the Central Santa Ynez Mountains Santa Barbara County, California*: California Division of Mines and Geology, Department of Conservation.
- Dorr H, Munnich K. 1990. <sup>222</sup>Rn flux and soil air concentration profiles in West Germany. Soil <sup>222</sup>Rn as tracer for gas transport in the unsaturated soil zone. *Tellus Ser B Chem Phys Meteorol* 42:20–8.
- Ehleringer JR, Buchmann N, Flanagan LB. 2000. Carbon isotope ratios in belowground carbon cycle processes. *Ecol Appl* 10:412–22.
- Elberling B. 2003. Seasonal trends of soil CO<sub>2</sub> dynamics in a soil subject to freezing. *J Hydrol* 276:159–75.
- Eswaran H, Berg EVD, Reich P. 1993. Organic carbon in soils of the world. *Soil Sci Soc Am J* 57:192–4.
- Fierer N, Schimel J, Holden P. 2003. Variations in microbial community composition through two soil depth profiles. *Soil Biol Biochem* 35:167–76.
- Gaudinski JB, Trumbore SE, Davidson EA, Zheng S. 2000. Soil carbon cycling in a temperate forest: Radiocarbon-based estimates of residence times, sequestration rates and partitioning of fluxes. *Biogeochemistry (Dordrecht)* 51:33–69.
- Gessler PE, Chadwick OA, Chamran F, Althouse L, Holmes K. 2000. Modeling soil-landscape and ecosystem properties using terrain attributes. *Soil Sci Soc Am J* 64:2046–56.
- Hendry M, Mendoza C, Kirkland R, Lawrence J. 1999. Quantification of transient CO<sub>2</sub> production in a sandy unsaturated zone. *Water Resources Res* 35:2189–98.
- Hillel D. 1998. *Environmental Soil Physics*. San Diego: Academic Press.
- Hooper B. 2003. *Spatial and temporal analysis of moisture and temperature as controls on soil respiration at the hillslope scale in California oak savanna* [M.S. dissertation]. University of California, Santa Barbara.
- Keller CK, Bacon D. 1998. Soil respiration and georespiration distinguished by transport analyses of vadose CO<sub>2</sub>, <sup>13</sup>CO<sub>2</sub>, and <sup>14</sup>CO<sub>2</sub>. *Global Biogeochem Cycles* 12:361–72.
- Khalil M, Rasmussen R, Shearer M. 1998. Flux measurements and sampling strategies: Applications to methane emissions from rice fields. *J Geophys Res* 103:25211–9.
- Millington R, Shearer R. 1971. Diffusion in aggregated porous media. *Soil Sci* 111:372–8.
- Nazaroff W. 1992. Radon transport from soil to air. *Rev Geophys* 30:137–60.
- Pumpanen J, Ilvesniemi H, Hari P. 2003. A process-based model for predicting soil carbon dioxide efflux and concentration. *Soil Sci Soc Am J* 67:402–13.
- Raich JW, Schlesinger WH. 1992. The global carbon dioxide flux in soil respiration and its relationship to vegetation and climate. *Tellus Ser B Chem Phys Meteorol* 44:81–99.
- Rambal S, Debussche G.. 1995. Water balance of Mediterranean ecosystems under a changing climate. In: Moreno J, Oechel W, eds. *Global Change and Mediterranean-Type Ecosystems*. New York: Springer-Verlag. p 386–407.
- Richter D, Markewitz D. 1995. How deep is soil? *Bioscience* 45:600–9.
- Rovira P, Vallejo VR. 1997. Organic carbon and nitrogen mineralization under Mediterranean climatic conditions: The effects of incubation depth. *Soil Biol Biochem* 29:1509–20.
- Rustad LE, Huntington TG, Boone RD. 2000. Controls on soil respiration: Implications for climate change. *Biogeochem* 48:1–6.
- Schimel DS. 1995. Terrestrial ecosystems and the carbon cycle. *Global Change Biol* 1:77–91.
- Schimel DS, Braswell BH, Holland EA, McKeown R, Ojima DS, Painter TH, Parton WJ, Townsend AR. 1994. Climatic, edaphic, and biotic controls over storage and turnover of carbon in soils. *Global Biogeochem Cycles* 8:279–93.
- Schlesinger W. 1991. *Biogeochemistry: An Analysis of Global Change* New York: Academic Press.
- Shipman GE. 1972. *Soil Survey of Santa Barbara County*, USDA Soil Conservation Service..
- Soil Survey Staff1996a. *Keys to Soil Taxonomy* 7 ed. Lincoln, NE: USDA-NRCS.
- Soil Survey Staff1996b. *Soil survey laboratory methods manual, version 3.0* Lincoln, NE: USDA-NRCS.
- Solomon DK, Cerling TE. 1987. The annual carbon dioxide cycle in a montane soil: observations, modeling, and implications for weathering. *Water Resources Res* 23:2257–65.

- Stranden E, Kolstad A, Lind B. 1984. The influence of moisture and temperature on radon exhalation. *Radiat Protect Dosim* 7:55–8.
- Stuiver M, Polach H. 1977. Reporting of <sup>14</sup>C data. *Radiocarbon* 19:355–63.
- Stumm W, Morgan J. 1981. *Aquatic Chemistry: An Introduction Emphasizing Chemical Equilibria in Natural Waters* 2nd ed. New York: John Wiley & Sons.
- Thorstenson D, Pollock D. 1989. Gas transport in unsaturated zones: Multicomponent systems and the adequacy of Fick's law. *Water Resources Res* 25:477–507.
- Trumbore S. 2000. Age of soil organic matter and soil respiration: Radiocarbon constraints on belowground C dynamics. *Ecol Appl* 10:399–411.
- Vogel J. 1992. A rapid method for preparation of biomedical targets for AMS. *Radiocarbon* 34:344–50.
- Wood W, Petraitis M. 1984. Origin and distribution of carbon dioxide in the unsaturated zone of the southern high plains of Texas. *Water Resources Res* 20:1193–208.
- Wood B, Keller C, Johnstone D. 1993. In situ measurement of microbial activity and controls on microbial CO<sub>2</sub> production in the unsaturated zone. *Water Resources Res* 29:647–59.
- Yavitt JB, Fahey TJ, Simmons JA. 1995. Methane and carbon dioxide dynamics in a northern hardwood ecosystem. *Soil Sci Soc Am J* 59:796–804.
- Yoshikawa S, Hasegawa S. 2000. Diurnal and seasonal changes in CO<sub>2</sub> concentration and flux in an Andisol and simulation based on changes in CO<sub>2</sub> production rate and gas diffusivity. *Jpn Agric Res* 34:1–13.